

1 | **Orographic-Topographic** and vegetation effects on snow
2 **accumulation in the southern Sierra Nevada: a statistical**
3 **summary from LidarDAR data**

4
5 **Z. Zheng¹, P. B. Kirchner^{2,3}, R. C. Bales^{1,4}**

6 [1] Department of Civil and Environmental Engineering, UC Berkeley, Berkeley, CA, USA

7 [2] Joint Institute for Regional Earth System Science and Engineering, Pasadena, CA, USA

8 [3] Southwest Alaska Network, National Park Service, Anchorage, AK, USA

9 [4] Sierra Nevada Research Institute, UC Merced, Merced, CA, USA

10

11 Correspondence to: Z. Zheng (zeshi.z@berkeley.edu)

12 Abstract

13 Airborne light detection and ranging (Lidar~~DAR~~) snow-on and snow-off measurements collected
14 in the southern Sierra Nevada near peak snow accumulation and in the snow-free season in the
15 2010 water year were analyzed for ~~orographic-topographic~~ and vegetation effects on snow
16 accumulation ~~during the winter season~~. Combining point-cloud data from four sites separated by
17 10 to 64 km, ~~and together covering with total surveyed area~~ over 106 km², it was observed in that
18 the mixed-conifer forest the percent of pixels with snow-depth measurements is sensitive to the
19 sampling resolution used in processing the point cloud. This is apparently due to Lidar not
20 receiving returns from under the denser canopy. From the 1-m gridded data, it was observed that
21 in addition to elevation effects, snow depth has a strong dependency on slope, aspect and canopy
22 penetration fraction. A multivariate linear model built using all physiographic variables
23 explained 15 to 25% more variability in snow depth than did a univariate linear model with
24 elevation as a single predictor. However, the weight that each physiographic variable exerted on
25 snow depth varied across different elevation ranges, as well as with different canopy-cover
26 amounts. The difference between mean snow depth measured in open area and under canopy
27 increased with elevation in rain-snow transition zone from 1500 to 1800 m and stabilized at
28 about 25 to 45 cm above about 2000 m elevation, with the range reflecting the effects of other
29 topographic variables. ~~area, the 1-m elevation band averaged snow depth in canopy gaps as a~~
30 ~~function of elevation increased at a rate of 15 cm per 100 m until reaching the elevation of 3300~~
31 ~~m. The averaged snow depth of the same elevation band from different sites matched up with~~
32 ~~minor deviation, which could be partially attributed to the variation in other topographic features,~~
33 ~~such as slope and aspect. As vegetation plays a role in the snow accumulation, the distribution of~~
34 ~~the vegetation was also studied and shows that the canopy coverage consistently decreased along~~

35 the elevation gradient from 80% at 1500 m to near 0% at above 3300 m. Also, the absolute
36 difference of the averaged snow depth between snow found in canopy gaps and under the canopy
37 increased with elevation, and decreased with canopy coverage disregarding the variation of other
38 topographic features. The influence from the forest density on snow accumulation was quantified
39 based on the snow depth residuals from 1-m elevation band averaged snow depth and the
40 attribute penetration fraction, which is the ratio of the number of ground points to the number of
41 total points per pixel of LiDAR data. The residual increases from -25 cm to 25 cm at the
42 penetration fraction range of 0% to 80%; and the relationship could be modeled by exponential
43 functions, with minor fluctuations along the gradient fraction of canopy and small deviation
44 between sites.

45 1. Introduction

46 In the western United States, ecosystem processes and water supplies for agricultural and
47 domestic use depend on the mountain snowpack ~~as is~~ the primary source of late-spring and early
48 summer streamflow ~~and is associated with agricultural and municipal water supplies~~ (Bales et al.,
49 2006). Knowledge of spring snowpack conditions within a watershed is essential if water
50 availability and flood peaks following the onset of melt are to be accurately predicted
51 (Hopkinson et al., 2001). Both topographic and vegetation factors are important in influencing
52 the snowpack conditions, as they closely interact with meteorological conditions to affect
53 precipitation and snow accumulation distribution in the mountains (McMillen, 1988; Raupach,
54 1991; Wigmosta et al., 1994). However, the distribution of mountain precipitation is poorly
55 understood at multiple spatial scales because it is governed by processes that are neither well
56 measured nor accurately predicted (Kirchner et al., 2014). Snow accumulation across the
57 mountains is primarily influenced by orographic processes, involving feedbacks between
58 atmospheric circulation and terrain (Roe, 2005; Roe and Baker, 2006). In most forested regions,
59 snow accumulation is highly sensitive to vegetation structure (Anderson, 1963; Revuelto et al.,
60 2015; Musselman et al., 2008), and canopy ~~snow~~-interception, sublimation and unloading results
61 in ~~smaller-less~~ accumulations of snow beneath the forest canopies in comparison with canopy
62 gaps (Mahat and Tarboton, 2013).

63 The Sierra Nevada is ideally suited for studying mountain snow distribution and related
64 hydrologic processes because it serves as a barrier to moisture moving inland from the Pacific,
65 ~~provides-has~~ an ideal mountainous-region orientation for producing orographic precipitation, and
66 thus exerts a strong influence on the upslope amplification of precipitation (Colle, 2004; Rotach
67 and Zardi, 2007; Smith and Barstad, 2004). Recent studies have revealed some insights of snow-

68 depth dependency on orographic and topographic effects in the Alps (Grünewald et al., 2013;
69 Grünewald, et al., 2014; Lehning et al., 2011), suggesting that similar studies could be extended
70 to the Sierra Nevada. And among the forested regions of the mountains, the mixed-conifer and
71 subalpine zones cover most of the high-elevation, seasonally snow-covered area. ~~The geographic,~~
72 ~~topographic, and vegetation conditions make the Sierra Nevada a natural laboratory in the~~
73 ~~western United States for studying mountain snow distribution and related hydrologic processes~~
74 ~~(Grünewald et al., 2013; Grünewald, et al., 2014; Lehning et al., 2011).~~

75 ~~In order to have a better knowledge of precipitation and snow accumulation in the Sierra~~
76 ~~Nevada,~~ Manual snow surveys, one-time surveys, and remote-sensing products are used to
77 estimate precipitation and snow accumulation in the Sierra Nevada and analyzed (Guan et al.,
78 2013). ~~In situ observations,~~ operational measurements of snow water equivalent (SWE) ~~were~~
79 ~~obtained~~ come from monthly manual snow surveys and daily snow pillow observations
80 (Rosenberg et al., 2011). Cost, data coverage, accuracy (Julander et al., 1998) and basin-scale
81 representativeness are issues for *in situ* monitoring of SWE in mountainous terrain (Rice and
82 Bales, 2010). Satellite-based remote sensing, such as MODIS, has been used to map snow
83 coverage in large or even global areas. ~~Fractional snow coverage, grain size and albedo have~~
84 ~~retrieved from MODIS data (Hall et al., 2002; Painter et al., 2009; Rittger et al., 2013), however~~
85 ~~the products do not fit catchment size studies owing to its low spatial resolution. However, it~~
86 ~~also~~ only provides snow-coverage information in canopy gaps, and no direct information on
87 snow depths (Molotch and Margulis, 2008). There is also the SNOW Data Assimilation Systems
88 (SNODAS) that integrate data from satellite and *in situ* measurements into a physical snowpack
89 model, which provides SWE and snow depth information estimates (Barrett, 2003). However,
90 since ~~Since the spatial resolution of SNODAS is 1 km and its products have~~ not been globally

91 broadly evaluated (Clow et al., 2012), its potential for studying the snow distribution in
92 mountainous areas remains uncertain. Also, owing to its 1-km spatial resolution, the snow depth
93 that SNODAS provides is a mixed representation of both open and canopy-covered areas.
94 ~~SNODAS could not be used for studying the snow distribution on catchment scale in the Sierra~~
95 ~~Nevada.~~An orographic-lift effect is observable in most of the above data (Howat and Tulaczyk,
96 2005; Rice et al., 2011), and a binary-regression-tree model using topographic variables as
97 predictors has also been used for estimating the snow depth in unmeasured areas (Erickson et al.,
98 2005; Erxleben et al., 2002; Molotch et al., 2005). However, regression coefficients could not be
99 estimated accurately for most of the predictors, except for elevation, and the consistency of the
100 orographic trend as well as the relative importance of these predictors is still unknown owing to
101 lacking representative measurements across different slopes, aspects and canopy conditions. And
102 the stability of the variance explained by the model also needs to be tested with denser
103 measurements.

104 In recent years, airborne ~~Lidar~~~~DAR~~ has been employed for high-spatial-resolution
105 distance measurements (Hopkinson et al., 2004), and has become an important technique to
106 acquire topographic data with sub-meter resolution and accuracy (Marks and Bates, 2000).
107 Therefore, ~~Lidar~~~~DAR~~ provides a potential tool to help understanding spatially distributed snow
108 depth across mountainous regions. With multiple returns from a single laser ~~beam~~~~pulse~~,
109 ~~Lidar~~~~DAR~~ has also been used to construct vegetation structures as well as observe conditions
110 under the canopy, which helps produce fine-resolution digital elevation models (DEMs),
111 vegetation structures, and snow-depth information. However, the snow depth under canopy can
112 not always be measured because of the signal-intensity attenuation caused by canopy
113 interception (Deems and Painter, 2006; Deems et al., 2006). A recent report applied a univariate-

114 regression model to the snow depth measured in open areas using Lidar; with a high-resolution
115 DEM used to accurately quantify the orographic-lift effect on the snow accumulation just prior to
116 melt (Kirchner et al., 2014). From this analysis it could be expected that Lidar data might also
117 help explain additional sources of snowpack distribution variability in complex, forested terrain.
118 ~~Even without LiDAR surveys, Erickson et al., (2005) and Erxleben et al., (2002) have~~
119 ~~used intensive *in situ* SWE measurements with binary regression tree, linear and nonlinear~~
120 ~~multivariate regression models for studying the topographic and vegetation controls on the~~
121 ~~spatial distribution of snow in the Colorado Rocky Mountains. But the studying sites were~~
122 ~~smaller than catchment size, and the results were site dependent as well as the sampling schemes~~
123 ~~have to be taken into consideration. Recent snow distribution modeling methods developed upon~~
124 ~~LiDAR measurements have been focused on fractal analysis and linear regression. Even the~~
125 ~~fractal distributions of snow depth do not vary with sites on local scale from 1 to 1000 m (Deems~~
126 ~~et al., 2006) and the topographic dependency of spatial snow depth distribution have been~~
127 ~~explored (Kirchner et al., 2014), consistency of the topographic and vegetation effects across~~
128 ~~sites still need to be addressed.~~

129 The objective of this work reported here is to improve our understanding of the ~~effect of~~
130 ~~elevation, slope, aspect and canopy cover topographic and vegetation effects~~ on snow
131 accumulation in the mixed-conifer forest. We investigated these by using ~~LiDAR~~ Lidar data
132 collected in four headwater ~~catchments areas~~ in the southern Sierra Nevada and address the
133 following three questions. First, is it possible to have snow-depth measurements in forested
134 mountain terrain from all pixels on a fine sampling resolution (1 to 5m) using Lidar data? If not,
135 how does the percentage of pixels measured change with the sampling resolution. Second, what
136 is the importance of slope, aspect and canopy penetration fraction on snow accumulation,

137 ~~relative to elevation; and are effects consistent across sites? Third, what is the snow-depth~~
138 ~~difference between open and canopy-covered areas; how does it change with elevation; and is the~~
139 ~~difference stable with respect to other topographic variables? First, is there a consistent~~
140 ~~orographic effect on snow accumulation across catchments; and what attributes could account for~~
141 ~~variability across and within sites? Second, what is the snow depth difference between canopy~~
142 ~~gaps, versus under canopy, along elevation; and is binary classification for canopy cover~~
143 ~~adequate to the differences? Third, how does forest density influence the snow accumulation in~~
144 ~~canopy gaps and if there are patterns, are they consistent across catchments?~~

145 **2. Methods**

146 **2.1 Study Areas**

147 ~~The Our~~ study areas ~~are~~is located in the southern Sierra Nevada, approximately 80 km
148 east of Fresno, California (Figure 1). ~~The f~~our headwater-catchment research areas, Bull Creek,
149 Shorthair Creek, Providence Creek, and Wolverton Basin were previously instrumented,
150 including meteorological measurements, in order to have a better knowledge of the hydrological
151 processes in this region (Bales et al., 2011; Hunsaker et al., 2012; Kirchner et al., 2014). The
152 sites were chosen as part of multi-disciplinary investigations at the Southern Sierra Critical Zone
153 Observatory, and are also the main instrumented sites in the observatory. Wolverton is
154 approximately 64 km ~~away in the~~ southeast ~~direction~~ of the other three sites (Figure 1) and is
155 located in Sequoia National Park. Both snow-on and snow-off airborne ~~LiDAR-Lidar~~ were flown
156 in 2010 (Table 1, ~~only later date collections were processed~~) over these sites. The elevation of
157 the survey areas ~~covers is~~ from 1600-m to 3500-m elevation, ~~over which~~ Vegétation density
158 generally decreases ~~with biotic zones of~~ in high-elevation subalpine forest, ~~and with Wolverton~~
159 also having a large area above treeline ~~in Wolverton~~ (Goulden et al., 2012). The precipitation has

160 historically been mostly snow in the cold and wet winters for elevations above 2000 m, and a
161 rain-snow ~~transition-mix~~ below 2000 m, where most of Providence is located. The comparison
162 between Providence and the other sites can help in accessing if observed trends are consistent
163 above and below the rain-snow transition. Also, various elevation spans of sampling sites is
164 important in understanding the stability of the relative importance of physiographic variables
165 across heterogeneous topography.

166 **2.2 Data Collection**

167 AllBoth airborne LiDAR surveys were performed by using Optech GEMINI Airborne
168 Laser Terrain Mapper. The scan angle and scan frequency were adjusted to ensure a uniform
169 along-track and across-track point spacing (Table 2), and six GPS ground stations were used for
170 determining aircraft trajectory. The snow-on survey date was close to April 1st, which is used by
171 operational agencies as the date of peak snow accumulation for the Sierra time. Since the snow-
172 on survey ~~lasted-required~~ four days to ~~finish data collection overcover~~ the four study areas, time-
173 series *in situ* snow-depth data measured continuously from Judd Communications ultrasonic
174 depth sensors ~~of the meteorological stations~~ at Providence, Bull and Wolverton were used to
175 estimate changes in snow depth during the survey period. for checking if precipitation had
176 occurred during survey dates and While no snow accumulation was observed, also taking
177 snowpack densification and melting observed from the time-series data were taken into
178 considerations (Hunsaker et al., 2012; Kirchner et al., 2014). The snow-off survey was
179 performed in August ~~when-after~~ snow ~~was-had~~ completely melted out in the study areas.

180 **2.3 Data Processing**

181 Raw ~~LiDAR-Lidar~~ datasets were pre-processed by NCALM and are available from the
182 NSF Open-Topography website (<http://opentopography.org>) in LAS format. The LAS point

183 clouds, including both canopy and ground-surface points, are stored and classified as ground
184 return and vegetation return. Each point is also attributed with the total number of returns and
185 position of all returns from its source laser pulsebeam. The 1-m resolution digital-elevation
186 models, generated from the LiDAR-Lidar point-cloud datasets, were downloaded from the
187 OpenTopography database and further processed in ArcMap 10.2 to generate 1-m resolution
188 slope, aspect, and northness raster products. Northness is an index for the potential amount of
189 solar radiation reaching a slope on a scale of -1 to 1, calculated from:

190

$$191 \quad N = \sin(S) \times \cos(A), \quad (1)$$

192

193 where N is the northness value; S is the slope angle of the terrain; and A is the aspect angle.

194 Northness is also the same as the aspect intensity (Kirchner et al., 2014) with 0° focal aspect.

195 Since in this analysis the snow-depth comparison is only discussed between north and south

196 facing slopes, northness is used instead of aspect intensity for simplification. To construct the

197 vegetation structure from LiDAR-Lidar data, points that are from the first return of the laser

198 pulsebeam are used to generate 1-m gridded digital-surface models. And 1-m resolution canopy-

199 height models were was built by subtracting the digital-elevation models from the digital-surface

200 models.

201 The snow depths were calculated directly from the snow-on LiDAR-Lidar data. By

202 referring to canopy-height models, all ground points in snow-on LiDAR-Lidar datasets were

203 classified as under canopy or in canopy gaps. That is, if the point was undercoincident with

204 canopy of >2-m height, it was classified as under canopy, and otherwise in a canopy gap. After

205 classification, snow depths were calculated by subtracting the values in the digital-elevation

206 model from the snow-on point-measurement values. The calculated point snow-depth data were
207 further assigned into 1-m raster pixels, averaged within each pixel, formatted and then gap filled
208 by interpolation with pixel values around it. Since the measurements collected under canopy
209 were insufficient within each pixel (Figure 2) and varied across the transition from the tree trunk
210 to the edge of the canopy, interpolation was not applied to data under the canopy. The error rate
211 of the calculated snow depth should be mainly from the instrumental elevation error, which is
212 about 0.10 m (Kirchner et al., 2014; Nolan et al., 2015).

213 **2.4 Penetration Fraction**

214 The open-canopy fraction is a factor that represents the forest density above a given
215 pixel and is ~~often~~ used to describe the influence of vegetation on snow accumulation and melt.
216 However there is no algorithm to directly extract this information from LiDAR-Lidar data. Here
217 we use a novel approach we call penetration fraction to approximate the open-canopy fraction
218 from the LiDAR-Lidar point cloud. Penetration fraction is the ratio of the number of ground
219 points ~~to~~ number of total points within each pixel. Because the electromagnetic radiation
220 from both ~~the LiDAR-Lidar~~ and sunlight beams are intercepted by canopies, the open-canopy
221 fraction is used here as an index to represent the fraction of sunlight radiance received on the
222 ground under vegetation. Therefore, penetration fraction of LiDAR-Lidar is actually another
223 form of estimating the open-canopy fraction (Musselman et al., 2013). Penetration fraction was
224 calculated as the number of ground points divided by total points in each pixel (Figure 3a).
225 However, under-canopy vegetation can also intercept the LiDAR-Lidar beam causing a bias. To
226 eliminate this bias, the canopy-height model was used to check if the pixel was canopy covered
227 by using a threshold value of 2 m; and if not, the local penetration fraction of the pixel was reset
228 to 1 because the open-canopy fraction of a pixel could not be entirely represented by the

229 penetration fraction. A spatial moving-average process was applied using a 2-D Gaussian filter
230 with a radius of 5 m to account for the effect of the vegetation around each pixel. Finally, we
231 tested the sensitivity of smoothing results to the radius of the filter and found it is not sensitive
232 when the radius is greater than 1.5 m (Figure 3b).

233 **2.5 Statistical Analysis**

234 The 1-m resolution snow-depth raster datasets were resampled into 2-m, 3-m, 4-m and 5-
235 m resolution. The percentage of pixels with snow-depth measurements was calculated by using
236 the number of pixels with valid data divided by the total number of pixels inside each survey
237 area. The sensitivity of the percentage changes across different resampling resolutions and the
238 consistency of the percentages across study sites at the same resampling resolution were
239 analyzed by visualizing the percentages against sampling resolutions at all sites.

240 Using elevation, slope, aspect, ~~penetration fraction~~~~vegetation structure~~ and snow _depth
241 retrieved from ~~LiDAR-Lidar~~ measurements, ~~orographic-topographic~~ and vegetation effects on
242 snow ~~pack~~ accumulation were ~~analyzed statistically~~observed using residual analysis. Owing to
243 orographic effects, there is increasing precipitation along an increasing elevation gradient in this
244 area (Kirchner et al., 2014). Therefore, elevation was selected as the primary variable
245 ~~topographic attribute~~to fit the linear regression model for calculating the residual of snow depth.
246 All snow-depth measurements from ~~LiDAR-Lidar~~ were first separated by either under canopy or
247 in canopy gaps, and then were binned by elevation of the location where they were measured,
248 with a bin size of 1-m elevation. As each elevation band had hundreds of snow-depth
249 measurements after binning, the average of all snow depths was chosen as the representative
250 snow depth, and the standard deviation calculated to represent the snow-depth variability within
251 each elevation band. ~~Correlation-c~~oefficients of determination between snow depth and

252 elevation of each site were calculated by linear regression. The fitted linear regression model of
253 each site was applied to the DEM to estimate the snow depth. The residual of snow depth was
254 calculated by subtracting the modeled snow depth from Lidar-measured snow depth. The slope,
255 aspect and penetration fraction were binned into 1° slope, 1° aspect, and 1% penetration-fraction
256 bins. In this study we treat penetration fraction as a physiographic variable and snow-depth
257 residuals corresponding to each bin of each physiographic variable were averaged and visualized
258 along the variable gradient to check the existence of these physiographic effects.~~Northness and~~
259 ~~slope were also averaged by elevation band for cross comparison. The differences of averaged~~
260 ~~snow depth between in canopy gaps and under canopy areas were calculated for each elevation~~
261 ~~band and cross compared with the vegetation fraction, northness and slope.~~

262 ~~——— To account for effects other than elevation in the snow depth, a linear regression model of~~
263 ~~snow depth and elevation was applied to the digital elevation data to estimate snow depth. The~~
264 ~~differences between the estimated and LiDAR measured snow depths were further investigated,~~
265 ~~with respect to slope, aspect and penetration fraction, by binning the snow depth difference into~~
266 ~~1° slope and aspect bins and 1% penetration fraction bins. The difference values within each bin~~
267 ~~were averaged and the standard deviations were calculated.~~

268 For the variables found to correlate with the snow accumulation, the relative importance
269 of each variable was calculated using the Random Forest algorithm (Breiman, 2001; Pedregosa
270 and Varoquaux, 2011). A multivariate linear regression model was also fitted into all
271 physiographic variables to calculate the regression coefficients, which could be used as the
272 quantification of the effect on snowpack distribution from the variable.

273 To calculate the snow-depth difference between open and canopy-covered area along an
274 elevation gradient, the 1-m resolution snow-depth data of the two conditions, open and canopy-

275 covered, were smoothed separately against elevation using locally weighted scatterplot
276 smoothing (LOESS) (Cleveland, 1979). The snow-depth difference was then calculated by
277 subtracting the smoothed canopy-covered snow depth from that in open.

278 3. Results

279 The percentage of pixels that have snow-depth data measured is highly sensitive to the
280 sampling resolution used in processing the Lidar point cloud, which is about 65 to 90% with 1-m
281 resolution and gradually increases to 100% at 5-m resolution (Figure 4). Note that the percentage
282 increases in going from the lower to higher elevation sites, consistent with local forest density
283 decreasing with elevation.

284 The snow depth ~~estimated~~ in canopy gaps shows a ~~strong~~-consistent linear trend with
285 elevation across all sites (Figure 5a). The variability (Figure 5b) is highest at about 1500 m, and
286 gradually decreases within rain-snow transition until elevation reaches 2000 m. However, at
287 above 2000 m, the trends of variability changing along elevation gradient vary across sites. ~~ey-of~~
288 ~~distribution patterns and variability across the four sites (Figure 4a, 4b).~~ In general, snow depth is
289 linearly correlated with elevation at all sites, both in the open area and under the canopy. ~~snow~~
290 ~~depth under the canopy is consistently less than in the canopy gaps (Figure 5a).~~ Note that values
291 at the upper or lower ends of elevation at each site have few pixels and maybe less representative
292 of the value of physiographic attributes in the study areas (Figure 5c). The forested area, of all
293 four sites combined, spans the rain-snow transition zone in mixed conifer through subalpine
294 forest to significant areas above treeline. ~~The snow depth difference between canopy gaps and~~
295 ~~under canopy varies with elevation, generally increasing from near zero at 1500 m, where there~~
296 ~~is little snow but dense canopy, to 40 cm in the range of 2000-2400 m, and varying from near~~
297 ~~zero to 60 cm at higher elevation where snow is deeper and canopy less dense.~~

298 For each individual site, ~~the a~~ least-squares linear regressions of snow depth ~~and versus~~
299 elevation ~~were was~~ used to investigate the spatial variability of snow ~~_depth across sites~~. The
300 median elevation of the three sites increases ~~in going~~ from Providence to Bull to Shorthair. The
301 lowest elevation at Providence Creek is less than goes down to 1400 m, and snow depth
302 increases steeply in this region at a rate of 38 cm per 100 m in canopy gaps open areas and 28 cm
303 per 100 m under the canopy. Bull Creek has an elevation range of 2000-2400 meters, which is
304 slightly higher than Providence, and has snow depth increasing at 21 cm per 100 m in canopy
305 gaps open areas and 19 cm per 100 m under the canopy. For Shorthair Creek site, which is the
306 highest of the three, the snow depth increases at 17 cm per 100 m in canopy gaps open areas and
307 16 cm per 100 m under the canopy. Wolverton is 64 km further south and spans a wide elevation
308 range, going from the rain-snow transition in mixed conifer, to subalpine forest, to some area
309 above treeline. The average snow-depth increase is smallest among all four study sites, 15 cm
310 per 100 m in canopy gaps and 13 cm per 100 m under the canopy. Unlike the other three lower-
311 elevation sites, the snow depth at Wolverton site decreases ~~after above~~ 3300-m elevation.
312 However The amount of area above this elevation is relatively small, and factors such as wind
313 redistribution and the exhaustion of perceptible water can also affect snow depth at these
314 elevations (Kirchner et al., 2014). ~~the amount of area above this elevation also drops off steeply.~~

315 The residuals for the snow in the open areas were further analyzed for effects of slope,
316 aspect and penetration fraction. The snow-depth residual decreases about 10 to 40 cm as slope
317 angle increases from 0° to 60°; and the residual decreases around 50 to 100 cm in going from
318 north-facing to south-facing slopes (Figure 6a, 6b). More interestingly, the topographic effect
319 can be seen from the color pattern of northness observed in the scatterplots (Figure 7a, 7b). The
320 residual increases about 40 to 60 cm as penetration fraction increases from 0% to 80% (Figure

321 6C). Considering all of these variables together, elevation is the most important variable at all
322 sites except for Shorthair, which has a relatively small elevation range (Figure 8). Aspect exerts a
323 stronger influence than do slope and penetration fraction in open areas. However, for under-
324 canopy areas, penetration is more dominant than aspect at two sites. The multivariate regression
325 model was fitted to the data with aspect transformed into 0° to 180° range (north to south).
326 Fitted models could be represented as the following two equations for open area and under
327 canopy respectively,

328 $SD = 0.0011 \times Elevation - 0.0112 \times Slope - 0.0057 \times Aspect + 0.1802 \times Penetration \quad (2)$

329 $SD = 0.0009 \times Elevation - 0.0128 \times Slope - 0.0046 \times Aspect + 0.9891 \times Penetration \quad (3)$

330 where *SD* is snow depth and p-values of all regression coefficients of the two models are all
331 smaller than 0.01.

332 The snow-depth difference between open and canopy-covered area was calculated with
333 elevation from locally smoothed snow depth (Figure 7). It ~~The snow depth difference between~~
334 ~~canopy gaps and under canopy varies with elevation, generally increasing~~es from near zero at
335 ~~1500 m, where there is little snow but dense canopy, to 40 cm in the range of 2000-2400 m, and~~
336 ~~varies~~ing from near zero to 60 cm at higher elevations where snow is deeper and the canopy
337 ~~less dense~~. It is apparent that the snow-depth difference increases with elevation in the
338 rain-snow transition zone, but lacks a clean pattern along either elevation gradient or penetration-
339 fraction gradient when the elevation is higher.

340 ~~A visual inspection of the pattern of snowpack distribution with elevation for all sites~~
341 ~~shows a consistent pattern (Figure 4). Especially for the elevation range where Providence and~~
342 ~~Wolverton overlap, the patterns of snow depth change are the same for both sites, with the only~~
343 ~~difference being Wolverton snow depth is consistently less than that in Providence, which is~~

344 likely due to a small amount of densification that occurred between the two acquisitions (Table 1)
345 observed from depth sensors.

346 ~~At higher elevations, vegetation coverage decreases consistent with lower temperature,~~
347 ~~and soil depth. By cross-comparing the vegetation fraction and snow depth difference (Figure 5a,~~
348 ~~5b), similar patterns were observed at all sites along elevation gradient. Also, for most of the~~
349 ~~elevation range investigated, the snow depth difference was either increasing or remaining~~
350 ~~constant, except for 2300 to 2500 m at Wolverton, where the snow depth difference drops~~
351 ~~drastically, which may be explained by steeper and more southerly exposed slopes (Kirehner et~~
352 ~~al., 2014) (Figure 6).~~

353 ~~The snow depth residual deviation from a linear increase with elevation, investigated~~
354 ~~versus penetration fraction (Figure 7), indicates how the density of vegetation affects the snow-~~
355 ~~depth accumulation in canopy gaps. For all sites, the snow depth residuals increase with~~
356 ~~penetration fraction, with bias across sites and fluctuations at higher penetration fractions.~~

357

358 **4. Discussion**

359 **4.1 Sensitivity of measurements to sampling resolution**

360 The results of the percentage of pixels with snow depth measured from Lidar data at
361 different sampling resolutions illustrate that even high-density airborne Lidar measurements do
362 not have 100% coverage of the surveyed area at 1-m resolution, especially in densely forested
363 areas. According to the snow-depth difference between snowpack in open areas and under
364 canopy, the trade-off between accuracy and coverage happens when adjusting the resolution; and
365 lower sampling resolutions can introduce overestimation into the results. This is because upon
366 averaging, sub-pixel area under the canopy that was not measured is represented by the open that

367 ~~is measured, introducing an overestimation error into the averaged snow depth of the pixel.~~
368 ~~Therefore, the sampling resolution for processing the Lidar point cloud needs to be chosen~~
369 ~~according to the objective and accuracy tolerance of the study.~~

370 ~~—— The overall increasing trend of precipitation with elevation observed from airborne~~
371 ~~LiDAR data is consistent with the orographic effect on precipitation (Roe, 2005; Roe and Baker,~~
372 ~~2006) and less snow accumulation was observed under vegetation at all sites. The decrease in~~
373 ~~under canopy snow is consistent with previous work using ground-based data (Bales et al. 2011,~~
374 ~~Musselman et al. 2008, and Varhola et al. 2010). Finally, the penetration fraction explained part~~
375 ~~of the snow depth residual of the linear model between snow depth and elevation.~~

376 **4.14.2 Orographic-Physiographic effect on snow accumulation**

377 Below 3300 m, the increasing trend of snow accumulation with elevation was observed
378 for all sites (Figure 54). Linear regression is applicable to model the relationship between snow
379 depth and elevation when the study area has a broad elevation range. ~~This holds true for all of~~
380 ~~our sites with the exception of Shorthair, where the elevation range is about 200 m and As~~
381 ~~indicated in Table 3, the correlation coefficient of determination for this linear model used for~~
382 ~~Shorthair site is much smaller than the other three sites, which have ranges greater than 500 m.~~
383 ~~The other three sites all have elevation range larger than 500 m; however the elevation spans~~
384 ~~around 200 m at Shorthair site.~~ The bias of mean snow depth in the same elevation band between
385 different sites is acceptable if the standard error is being added or subtracted from the mean
386 (Figure 54a, 54b). The data-collection time, spatial variation and variations of other topographic
387 features should introduce bias across sites. However, as data-collection time only differs a few
388 days, *in situ* snow-depth sensor data suggest that the melting and densification effect ~~should~~
389 ~~be~~ under 2 cm (https://czo.ucmerced.edu/dataCatalog_sierra.html). Spatial variations at

390 1800-2000 m elevations between Providence and the further—south Wolverton site appear to
391 have a consistent bias, with less precipitation falling in the southerly location. As for other
392 topographic variables, the observation of a slope effect, shown as the trend lines in Figure 6a and
393 the negative regression coefficients of the two linear models, could be explained by steeper
394 slopes having higher avalanche potential, fewer trees and thus more wind; and thus some snow is
395 more likely to be lost from these slopes. Snowpack located in south-facing slopes receives higher
396 solar radiation, with the snowmelt being accelerated (Kirchner et al., 2014). This explains the
397 trends observed in Figure 6b and the negative regression coefficients of the multivariate models.
398 Although Lidar has measurement errors caused by slope and aspect (Baltsavias, 1999; Deems et
399 al., 2013; Hodgson and Bresnahan, 2004), error is not able to be quantified and traced back to
400 each variable and we assumed its influence on the trends could be neglected. As canopy
401 interception results in reduced snow depth under canopy, the snow-depth residuals are found
402 increasing with penetration fraction and the regression coefficients are positive (Figure 6c). The
403 multivariate linear regression model built from the Lidar data is a significant improvement, as
404 the variability of the snowpack distribution could explain 15 to 25% more than the univariate
405 linear regression model with elevation as the only predictive variable (Table 4) and the
406 estimation bias has a narrower distribution (Figure 9a, 9b). Also, fitting an individual linear
407 model for each site is slightly better than using a general model with all sites' data involved
408 (Figure 9c, d) and it might be because that an individual model could capture regional micro-
409 climate within the site better than a general model. The opposite trend of the relative importance
410 of predictive variables observed in Shorthair is because it is a relatively flat site (Figure 1, Figure
411 8), which implies that topographic variables other than elevation need to be focused more when
412 studying about areas with small elevation ranges in future works. For other topographic features,

413 ~~Kirehner et al. (2014) proposed that northness and slope should have negative effects on snow~~
414 ~~accumulation. They noted that northness is positively correlated with solar radiation, and thus~~
415 ~~ablation, and northeastness deposition from prevailing winds. Steeper slopes also have has higher~~
416 ~~avalanche potential and snow is more likely to fall off from these slopes. Across the elevation~~
417 ~~range that we studied, the snow depth is globally smaller at Wolverton than all other sites;~~
418 ~~however the northness and slope are globally higher at Wolverton, which is consistent with the~~
419 ~~northness and slope effects on snow accumulation could exist. Also, the separate investigations~~
420 ~~on slope and aspect (Figure 6) show that smaller snow depth residuals could be observed on~~
421 ~~steeper or more southerly exposed slopes, which further proved the existence of the northness~~
422 ~~effect. From Figure 2 we also need to notice that each site has about 10% to 24% of total~~
423 ~~surveyed area does not have point return because of canopy interception. Thus the statistical~~
424 ~~results are representative but not conclusive of surveyed sites.~~

425 **4.24.3 Vegetation effects on snow accumulation along elevation**

426 _____

427 Under-canopy snow distribution is governed by multiple factors that affect the energy
428 environment, as observed by melting (Essery et al., 2008; Gelfan et al., 2004) and accumulation
429 rates (Pomeroy et al., 1998; Schmidt and Gluns, 1991; Teti, 2003). Our results show different
430 responses when comparing the snow-depth difference between open and canopy-covered areas
431 between study sites (Figure 7c). In the rain-snow transition zone from 1500 to 2000 m of
432 Providence we see a sharp linear increase between open and under-canopy accumulation that is
433 likely governed by the under-canopy energy environment and the canopy-interception effect on
434 precipitation, which accelerate snowmelt and prevent accumulation of under-canopy snow.
435 Above 2000 m, the snow-depth difference observed at Bull and Shorthair stabilized around 40

436 cm and 20 cm respectively, with fluctuations less than 10 cm along elevation. The snow depth in
437 open areas is increasing 2 cm / 100m to 12 cm / 100m steeper than snow depth in under-canopy
438 areas (Table 3). Schmidt and Gluns, (1991) found that the snow intercepted by canopy increases
439 with cumulative snowfall and the interception would saturate when the precipitation is heavy
440 enough. Therefore, in our study sites, with more snow intercepted at higher elevation, the snow-
441 depth increasing slope of under-canopy observations is gentler than open areas. Breaking from
442 this pattern, the large dip in snow-depth difference, down to 10 cm, observed at Wolverton at
443 elevations of 2250 - 2750 m deviates from the 35-40 cm plateau. Also, the snow-depth difference
444 at Shorthair stabilizes around 20 cm, which is 20 cm lower than the stabilized value at Bull.
445 Based on the scatterplot in Figure 7a and 7b that color coded by northness, at elevation range of
446 2300 m to 2700 m, there are a lot more data points with both low snow depth and extremely
447 negative northness in the open area than under the canopy, which implies that anisotropic
448 distribution of other topographic variables is affecting the snow-depth difference. This is further
449 shown by filtering out the data points not within a small certain range (-0.1 to 0.1) of northness,
450 and then reproducing Figure 7c using the filtered data. As presented in Figure 10, it is apparent
451 that the large dip at Wolverton is flattened out to a canopy effect of around 25-45 cm as the
452 topographic effect is filtered out. Thus a sigmoidal function was used to characterize the snow-
453 depth difference changes with elevation excluding topographic interactions. The interactions
454 between topographic variables and vegetation is most likely attributable to the under-canopy
455 snowpack being less sensitive to solar radiation versus snowpack in the open area (Courbaud et
456 al., 2003; Dubayah, 1994; Essery et al., 2008; Musselman et al., 2008, 2012).

457 In spite of filtering the topographic effect, there is still about a 20-cm magnitude of
458 fluctuation in the snow-depth difference, which might be attributed to various clearing sizes of

459 open area at different locations and various vegetation types in the forests (Hedstrom and
460 Pomeroy, 1998; Pomeroy et al., 2002; Schmidt and Gluns, 1991), however, these features of the
461 sites are not able to be explored from this Lidar data set.

462 ~~———The difference of averaged snow depth between open and under canopy areas increases~~
463 ~~with elevation as vegetation coverage decreases (Figure 5a, 5b). We found that a high density of~~
464 ~~vegetation exerts a negative influence on snow accumulation in canopy gaps, which makes the~~
465 ~~snow depth difference less significant at lower elevations. With precipitation increasing along~~
466 ~~the elevation gradient, the difference of snow depth between open and canopy covered areas also~~
467 ~~increases; and in more densely forested areas, even though the open area does not have canopy~~
468 ~~right above the ground (Hedstrom and Pomeroy, 1998; Pomeroy et al., 2002; Schmidt and Gluns,~~
469 ~~1991) they can still be influenced by the canopies around them. Golding and Swanson (1986)~~
470 ~~found that the difference increased with clearing size, caused by snow ablation as well as direct~~
471 ~~solar radiation reaching the snowpack. Another cause of this effect could be traced back to how~~
472 ~~precipitation drops on the ground. As precipitation has both horizontal and vertical velocities, in~~
473 ~~a densely forested area a small fraction of snowflakes or raindrops would be intercepted by the~~
474 ~~vegetation, not only vertically, but also horizontally. Therefore, the snow accumulated in the~~
475 ~~open area that is surrounded by dense vegetation would actually be smaller than the snow~~
476 ~~accumulated in a wide open area. This is also consistent with the finding that areas at the drip~~
477 ~~edge have snow depth values, intermediate between under canopy and in the open (Bales et al.,~~
478 ~~2011). Thus in the more open forests at higher elevation, the under canopy and in canopy gap~~
479 ~~allow for greater snow depth differences. Since the differences could change in different forest~~
480 ~~conditions and also under the effect of drip edge transitions, binary classification of in canopy~~
481 ~~gaps and under canopy does not work for quantifying differences in snow accumulation.~~

482 — Furthermore, the pattern could be altered as some other topographic feature varies. We
483 observed a sudden drop of snow depth difference in the elevation range of 2300-2500 m at
484 Wolverton from Figure 5a. By visually inspecting the vegetation pixel percentage, northness,
485 and slope along the elevation gradient (Figure 4d, 5b, 5c), it is observed that the vegetation pixel
486 percentage decreases constantly at a low rate and northness decreases from positive to negative
487 (north dominant to south dominant); while the slope kept increasing significantly in this
488 elevation range. Dubayah (1994), Courbaud et al. (2003), and Essery et al. (2008) found that
489 slope is a dominant factor in modeling the solar radiation received by the soil when canopy
490 structures remain constant, and more solar radiation would be received on steeper south facing
491 slopes, which could be the cause of the snow depth difference decrease that we observed.

492 **4.3 Quantify vegetation effects on snow accumulation**

493 — In the previous section, we reasoned that vegetation reduces snow accumulation in
494 canopy gaps by blocking the snow that in a less dense forest would fall to the ground. Vegetation
495 density is a significant factor (Teti, 2003), as we observed that snow depth difference increases
496 when vegetation fraction decreases. Figure 7 shows the quantification of the vegetation density
497 effects on the snow depth accumulation. Considering the blocking of snow from vegetation
498 (Pomeroy et al., 1998; Schmidt and Gluns, 1991), the vegetation density should be transformed
499 into open fraction that one could see from the given pixel. In this case, penetration fraction was
500 applied to represent percentage opening. As is shown in Figure 7a, the snow depth residual
501 differed from the linear increase with elevation is highly correlated with penetration fraction,
502 which implies that penetration fraction is a good indicator of vegetation effects on snow
503 accumulation. Moreover, the ranges of the snow depth residual are similar and the patterns of
504 snow depth residual changing against penetration fraction are consistent across sites, as the

505 ~~studied sites share similar vegetation structures and climate conditions (Fites Kaufman et al.,~~
506 ~~1970). The consistency of changing patterns supports the idea of modeling the relationship~~
507 ~~between vegetation density and snow depth so that the effects from vegetation on open area~~
508 ~~snow accumulation could be quantified.~~

509 **5. Conclusion_s**

510 As an advanced and promising remote-sensing technology, Lidar is able to measure snow
511 depth of 100% survey area at 5-m sampling resolution however the accuracy is still left to be
512 evaluated because of lacking enough representative measurements under the canopy. A 1-m
513 resolution processed Lidar data set is more accurate but the percentage of pixels with
514 measurements is much less than 100%.

515 Using processed Lidar data sampled at 1-m resolution, averaged snow depth within each
516 1-m elevation band shows a strong correlation with elevation at all sites, indicating that snow
517 accumulation in the southern Sierra Nevada is primarily affected by orographic lift. Snow-depth
518 residuals calculated by de-trending the elevation dependency are correlated with slope, aspect
519 and penetration fraction, which shows the effect of additional physiographic variables on snow
520 accumulation other than elevation. The relative importance of these variables in predicting snow
521 depth implies that other than elevation, aspect affects snow-accumulation and retention more in
522 open areas, while penetration fraction is as important as aspect for snow under the canopy. More
523 significantly, a multivariate linear regression model fitted with variables for slope, aspect and
524 canopy penetration fraction explains 15 to 25% more snow-depth variability than using elevation
525 as the only predictive variable, suggesting multiple predictive variables will be more effective for
526 quantifying the water equivalent in the Sierra Nevada at peak snow accumulation.

527 The snow-depth difference between open and canopy-covered areas increases in the rain-
528 snow transition elevation range and then stabilized around 25 to 45 cm at high elevation. Large
529 magnitude of fluctuations are presented at certain elevation ranges in Wolverton and Shorthair,
530 which is partially due to interactions from other topographic variables, evidence of which is
531 found by filtering the northness into a narrow band and which causes the fluctuations flattening
532 out.~~The regression analysis of snow depth versus terrain and vegetation attributes that are~~
533 ~~extracted from LiDAR show that snow accumulation in the southern Sierra Nevada is strongly~~
534 ~~affected by both the orographic effect and vegetation factors, and are consistent across the four~~
535 ~~sites studied. Comparing these results across sites reveals that the altitudinal effects on snow~~
536 ~~accumulation are consistent and globally linear, with a lapse rate of approximately 15 cm per 100~~
537 ~~m. By cross comparing between snow depth and other topographic features along the elevation~~
538 ~~gradient, we confirmed that the variability of snow depth, after de-trending the altitudinal effect,~~
539 ~~could be further explained by attributes such as slope and aspect. The characterization of snow-~~
540 ~~depth difference between open and canopy covered area, together with vegetation fraction, not~~
541 ~~only suggests that the snow depth difference increase along the elevation gradient is because of~~
542 ~~vegetation density decreasing, it also suggests that, penetration fraction can be used to~~
543 ~~quantitatively study vegetation effects on snow accumulation. Moreover, the analysis of the~~
544 ~~snow depth residual from the altitudinal trend and penetration fraction reveals that the vegetation~~
545 ~~effects on snow accumulation are consistent across the four study sites, implying that the effects~~
546 ~~could be quantified and modeled mathematically.~~

547 *Acknowledgements.* This material is based on data and processing services provided by the
548 OpenTopography Facility with support from the National Science Foundation under NSF Award
549 Numbers 1226353 & 1225810. Research was supported by the National Science Foundation
550 under NSF Award Numbers 1331939 & 1239521. We acknowledge the helpful comments from
551 Q. Guo, A. Harpold, and N.P. Molotch, also Q. Guo and J. Flanagan for providing canopy height
552 model data.

553 **Reference**

- 554 Anderson, H. W.: Managing California's Snow Zone Lands for Water, Pacific Southwest For.
555 Range Exp. Station. Berkeley, CA, 34, 1963.
- 556 Bales, R. C., Molotch, N. P., Painter, T. H., Dettinger, M. D., Rice, R. and Dozier, J.: Mountain
557 hydrology of the western United States, *Water Resour. Res.*, 42(8), n/a–n/a,
558 doi:10.1029/2005WR004387, 2006.
- 559 Bales, R. C., Hopmans, J. W., O'Geen, A. T., Meadows, M., Hartsough, P. C., Kirchner, P.,
560 Hunsaker, C. T. and Beaudette, D.: Soil Moisture Response to Snowmelt and Rainfall in a
561 Sierra Nevada Mixed-Conifer Forest, *Vadose Zo. J.*, 10(3), 786, doi:10.2136/vzj2011.0001,
562 2011.
- 563 Baltsavias, E.: Airborne laser scanning: basic relations and formulas, *ISPRS J. Photogramm.*
564 *Remote Sens.*, (54), 199–214 [online] Available from:
565 [http://www2.geog.ucl.ac.uk/~mdisney/teaching/teachingNEW/PPRS/papers/Baltsavias_](http://www2.geog.ucl.ac.uk/~mdisney/teaching/teachingNEW/PPRS/papers/Baltsavias_Lidar.pdf)
566 [Lidar.pdf](http://www2.geog.ucl.ac.uk/~mdisney/teaching/teachingNEW/PPRS/papers/Baltsavias_Lidar.pdf), 1999.
- 567 Barrett, A. P.: National Operational Hydrologic Remote Sensing Center SNOW Data
568 Assimilation System (SNODAS) Products at NSIDC, NSIDC Spec. Rep. 11, (Natl. Snow and Ice
569 Data Cent.: Boulder, CO), 19, 2003.
- 570 Breiman, L. (University of C.: Random forest, *Mach. Learn.*, 45(1), 5–32,
571 doi:10.1023/A:1010933404324, 2001.
- 572 Cleveland, W. S.: Robust Locally Weighted Regression and Smoothing Scatterplots, *J. Am.*
573 *Stat. Assoc.*, 74(368), 829–836, doi:10.2307/2286407, 1979.
- 574 Clow, D. W., Nanus, L., Verdin, K. L. and Schmidt, J.: Evaluation of SNODAS snow depth and
575 snow water equivalent estimates for the Colorado Rocky Mountains, USA, *Hydrol. Process.*,
576 26(17), 2583–2591, doi:10.1002/hyp.9385, 2012.
- 577 Colle, B. a.: Sensitivity of Orographic Precipitation to Changing Ambient Conditions and
578 Terrain Geometries: An Idealized Modeling Perspective, *J. Atmos. Sci.*, 61(5), 588–606,
579 doi:10.1175/1520-0469(2004)061<0588:SOOPTC>2.0.CO;2, 2004.
- 580 Courbaud, B., De Coligny, F. and Cordonnier, T.: Simulating radiation distribution in a
581 heterogeneous Norway spruce forest on a slope, *Agric. For. Meteorol.*, 116(1-2), 1–18,
582 doi:10.1016/S0168-1923(02)00254-X, 2003.
- 583 Deems, J. S. and Painter, T. H.: Lidar measurement of snow depth: accuracy and error
584 sources, *Proc. 2006 Int. Snow Sci. Work. Telluride, Color. USA, Int. Snow Sci. Work.*, 330,
585 330–338, 2006.

586 Deems, J. S., Fassnacht, S. R. and Elder, K. J.: Fractal Distribution of Snow Depth from Lidar
587 Data, *J. Hydrometeorol.*, 7(2), 285–297, 2006.

588 Deems, J. S., Painter, T. H. and Finnegan, D. C.: Lidar measurement of snow depth: a review, *J.*
589 *Glaciol.*, 59(215), 467–479, doi:10.3189/2013JoG12J154, 2013.

590 Dubayah, R. C.: Modeling a solar radiation topoclimatology for the Rio Grande River Basin, *J.*
591 *Veg. Sci.*, 5(5), 627–640, doi:10.2307/3235879, 1994.

592 Erickson, T. a., Williams, M. W. and Winstral, A.: Persistence of topographic controls on the
593 spatial distribution of snow in rugged mountain terrain, Colorado, United States, *Water*
594 *Resour. Res.*, 41(4), 1–17, doi:10.1029/2003WR002973, 2005.

595 Erxleben, J., Elder, K. and Davis, R.: Comparison of spatial interpolation methods for
596 estimating snow distribution in the Colorado Rocky Mountains, *Hydrol. Process.*, 16(18),
597 3627–3649, doi:10.1002/hyp.1239, 2002.

598 Essery, R., Bunting, P., Rowlands, A., Rutter, N., Hardy, J., Melloh, R., Link, T., Marks, D. and
599 Pomeroy, J.: Radiative Transfer Modeling of a Coniferous Canopy Characterized by
600 Airborne Remote Sensing, *J. Hydrometeorol.*, 9(2), 228–241, doi:10.1175/2007JHM870.1,
601 2008.

602 Gelfan, a. N., Pomeroy, J. W. and Kuchment, L. S.: Modeling Forest Cover Influences on Snow
603 Accumulation, Sublimation, and Melt, *J. Hydrometeorol.*, 5(5), 785–803, doi:10.1175/1525-
604 7541(2004)005<0785:MFCIOS>2.0.CO;2, 2004.

605 Goulden, M. L., Anderson, R. G., Bales, R. C., Kelly, a. E., Meadows, M. and Winston, G. C.:
606 Evapotranspiration along an elevation gradient in California’s Sierra Nevada, *J. Geophys.*
607 *Res. Biogeosciences*, 117(3), 1–13, doi:10.1029/2012JG002027, 2012.

608 Grünewald, T., Stötter, J., Pomeroy, J. W., Dadic, R., Moreno Baños, I., Marturià, J., Spross, M.,
609 Hopkinson, C., Burlando, P. and Lehning, M.: Statistical modelling of the snow depth
610 distribution in open alpine terrain, *Hydrol. Earth Syst. Sci.*, 17(8), 3005–3021,
611 doi:10.5194/hess-17-3005-2013, 2013.

612 Grünewald, T., Bühler, Y. and Lehning, M.: Elevation dependency of mountain snow depth,
613 *Cryosph.*, 8(6), 2381–2394, doi:10.5194/tc-8-2381-2014, 2014.

614 Guan, B., Molotch, N. P., Waliser, D. E., Jepsen, S. M., Painter, T. H. and Dozier, J.: Snow water
615 equivalent in the Sierra Nevada: Blending snow sensor observations with snowmelt model
616 simulations, *Water Resour. Res.*, 49(August), 5029–5046, doi:10.1002/wrcr.20387, 2013.

617 Hedstrom, N. R. and Pomeroy, J. W.: Measurements and modelling of snow interception in
618 the boreal forest, *Hydrol. Process.*, 12(10-11), 1611–1625, doi:10.1002/(SICI)1099-

619 1085(199808/09)12:10/11<1611::AID-HYP684>3.0.CO;2-4, 1998.

620 Hodgson, M. E. and Bresnahan, P.: Accuracy of Airborne Lidar-Derived Elevation : Empirical
621 Assessment and Error Budget, *Photogramm. Eng. Remote Sensing*, 70(3), 331–339, 2004.

622 Hopkinson, C., Sitar, M., Chasmer, L., Gynan, C., Agro, D., Enter, R., Foster, J., Heels, N.,
623 Hoffman, C., Nillson, J. and Others: Mapping the spatial distribution of snowpack depth
624 beneath a variable forest canopy using airborne laser altimetry, *Proc. 58th Annu. East.
625 Snow Conf.*, 2001.

626 Hopkinson, C., Sitar, M., Chasmer, L. and Treitz, P.: Mapping snowpack depth beneath forest
627 canopies using airborne lidar., *Photogramm. Eng. Remote Sens.*, 70(3), 323–330, 2004.

628 Howat, I. M. and Tulaczyk, S.: Trends in spring snowpack over a half-century of climate
629 warming in California, USA, *Ann. Glaciol.*, 40, 151–156, doi:10.3189/172756405781813816,
630 2005.

631 Hunsaker, C. T., Whitaker, T. W. and Bales, R. C.: Snowmelt Runoff and Water Yield Along
632 Elevation and Temperature Gradients in California’s Southern Sierra Nevada¹, *JAWRA J.
633 Am. Water Resour. Assoc.*, 48(4), 667–678, doi:10.1111/j.1752-1688.2012.00641.x, 2012.

634 J. Revuelto, J. I. Lopez-Moreno, C. A.-M. and Vicente-Serrano, S. M.: Canopy influence on
635 snow depth distribution in a pine stand determined from terrestrial laser data, *Water
636 Resour. Res.*, doi:10.1002/2014WR016496, 2015.

637 Kirchner, P. B., Bales, R. C., Molotch, N. P., Flanagan, J. and Guo, Q.: LiDAR measurement of
638 seasonal snow accumulation along an elevation gradient in the southern Sierra Nevada,
639 California, *Hydrol. Earth Syst. Sci. Discuss.*, 11, 5327–5365, doi:10.5194/hessd-11-5327-
640 2014, 2014.

641 Lehning, M., Grünewald, T. and Schirmer, M.: Mountain snow distribution governed by an
642 altitudinal gradient and terrain roughness, *Geophys. Res. Lett.*, 38(19), 1–5,
643 doi:10.1029/2011GL048927, 2011.

644 Mahat, V. and Tarboton, D. G.: Representation of canopy snow interception, unloading and
645 melt in a parsimonious snowmelt model, *Hydrol. Process.*, 6336(December 2013), n/a–n/a,
646 doi:10.1002/hyp.10116, 2013.

647 Marks, K. and Bates, P.: Integration of high-resolution topographic data with floodplain
648 flow models, *Hydrol. Process.*, 14(July 1998), 2109–2122, doi:10.1002/1099-
649 1085(20000815/30)14:11/12<2109::AID-HYP58>3.0.CO;2-1, 2000.

650 McMillen, R. T.: An eddy correlation technique with extended applicability to non-simple
651 terrain, *Boundary-Layer Meteorol.*, 43(3), 231–245, doi:10.1007/BF00128405, 1988.

652 Molotch, N. P. and Margulis, S. a.: Estimating the distribution of snow water equivalent
653 using remotely sensed snow cover data and a spatially distributed snowmelt model: A
654 multi-resolution, multi-sensor comparison, *Adv. Water Resour.*, 31(11), 1503–1514,
655 doi:10.1016/j.advwatres.2008.07.017, 2008.

656 Molotch, N. P., Colee, M. T., Bales, R. C. and Dozier, J.: Estimating the spatial distribution of
657 snow water equivalent in an alpine basin using binary regression tree models: The impact
658 of digital elevation data and independent variable selection, *Hydrol. Process.*, 19(December
659 2004), 1459–1479, doi:10.1002/hyp.5586, 2005.

660 Musselman, K. N., Molotch, N. P. and Brooks, P. D.: Effects of vegetation on snow
661 accumulation and ablation in a mid-latitude sub-alpine forest, *Hydrol. Process.*, 22(15),
662 2767–2776, doi:10.1002/hyp, 2008.

663 Musselman, K. N., Molotch, N. P., Margulis, S. a., Kirchner, P. B. and Bales, R. C.: Influence of
664 canopy structure and direct beam solar irradiance on snowmelt rates in a mixed conifer
665 forest, *Agric. For. Meteorol.*, 161, 46–56, doi:10.1016/j.agrformet.2012.03.011, 2012.

666 Musselman, K. N., Margulis, S. a. and Molotch, N. P.: Estimation of solar direct beam
667 transmittance of conifer canopies from airborne LiDAR, *Remote Sens. Environ.*, 136, 402–
668 415, doi:10.1016/j.rse.2013.05.021, 2013.

669 Nolan, M., Larsen, C. and Sturm, M.: Mapping snow-depth from manned-aircraft on
670 landscape scales at centimeter resolution using Structure-from-Motion photogrammetry,
671 *Cryosph. Discuss.*, 9, 333–381, doi:10.5194/tcd-9-333-2015, 2015.

672 Pedregosa, F. and Varoquaux, G.: Scikit-learn: Machine Learning in Python, *J. Mach. ...*, 12,
673 2825–2830 [online] Available from:
674 <http://jmlr.csail.mit.edu/papers/volume12/pedregosa11a/pedregosa11a.pdf>, 2011.

675 Pomeroy, J. W., Parviainen, J., Hedstrom, N. and Gray, D. M.: Coupled modelling of forest
676 snow interception and sublimation, *Hydrol. Process.*, 12(15), 2317–2337,
677 doi:10.1002/(SICI)1099-1085(199812)12:15<2317::AID-HYP799>3.0.CO;2-X, 1998.

678 Pomeroy, J. W., Gray, D. M., Hedstrom, N. R. and Janowicz, J. R.: Prediction of seasonal snow
679 accumulation in cold climate forests, *Hydrol. Process.*, 16(18), 3543–3558,
680 doi:10.1002/hyp.1228, 2002.

681 Raupach, M. R.: Vegetation-atmosphere interaction in homogeneous and heterogeneous
682 terrain: some implications of mixed-layer dynamics, *Vegetatio*, 91(1-2), 105–120,
683 doi:10.1007/BF00036051, 1991.

684 Rice, R. and Bales, R. C.: Embedded-sensor network design for snow cover measurements
685 around snow pillow and snow course sites in the Sierra Nevada of California, *Water Resour.*

686 Res., 46(3), 1–13, doi:10.1029/2008WR007318, 2010.

687 Rice, R., Bales, R. C., Painter, T. H. and Dozier, J.: Snow water equivalent along elevation
688 gradients in the Merced and Tuolumne River basins of the Sierra Nevada, *Water Resour.*
689 *Res.*, 47(8), n/a–n/a, doi:10.1029/2010WR009278, 2011.

690 Roe, G. H.: Orographic Precipitation, *Annu. Rev. Earth Planet. Sci.*, 33(1), 645–671,
691 doi:10.1146/annurev.earth.33.092203.122541, 2005.

692 Roe, G. H. and Baker, M. B.: Microphysical and Geometrical Controls on the Pattern of
693 Orographic Precipitation, *J. Atmos. Sci.*, 63(3), 861–880, doi:10.1175/JAS3619.1, 2006.

694 Rosenberg, E. a., Wood, A. W. and Steinemann, A. C.: Statistical applications of physically
695 based hydrologic models to seasonal streamflow forecasts, *Water Resour. Res.*, 47(3), n/a–
696 n/a, doi:10.1029/2010WR010101, 2011.

697 Rotach, M. W. and Zardi, D.: On the boundary-layer structure over highly complex terrain:
698 Key findings from MAP, *Q. J. R. ...*, 133, 937–948, doi:10.1002/qj, 2007.

699 Schmidt, R. a. and Gluns, D. R.: Snowfall interception on branches of three conifer species,
700 *Can. J. For. Res.*, doi:10.1139/x91-176, 1991.

701 Smith, R. B. and Barstad, I.: A Linear Theory of Orographic Precipitation, *J. Atmos. Sci.*,
702 61(12), 1377–1391, doi:10.1175/1520-0469(2004)061<1377:ALTOOP>2.0.CO;2, 2004.

703 Teti, P.: Relations between peak snow accumulation and canopy density, *For. Chron.*, 79(2),
704 307–312, 2003.

705 Wigmosta, M. S., Vail, L. W. and Lettenmaier, D. P.: A distributed hydrology-vegetation
706 model for complex terrain, *Water Resour. Res.*, 30(6), 1665–1680,
707 doi:10.1029/94WR00436, 1994.

708

1 Table 1. LiDAR data collection information

	Snow-off flight date	Snow-on flight date	Area, km ²
Bull	August 15, 2010	March 24, 2010	22.3
Shorthair	August 13, 2010	March 23, 2010	6.8
Providence	August 5, 2010	March 23, 2010	18.4
Wolverton	August 13-15, 2010	March 21-22, 2010	58.9

2 Table 2. Flight parameters and sensor settings

Flight parameters		Equipment settings	
flight altitude	600 m	wavelength	1047 nm
flight speed	65 m s ⁻¹	beam divergence	0.25 mrad
swath width	233.26 m	laser PRF	100 kHz
Swath overlap	50%	scan frequency	55 Hz
point density	10.27 p m ⁻²	scan angle	±14°
Cross track res	0.233 m	scan cutoff	3°
Down track res	0.418 m	scan offset	0°

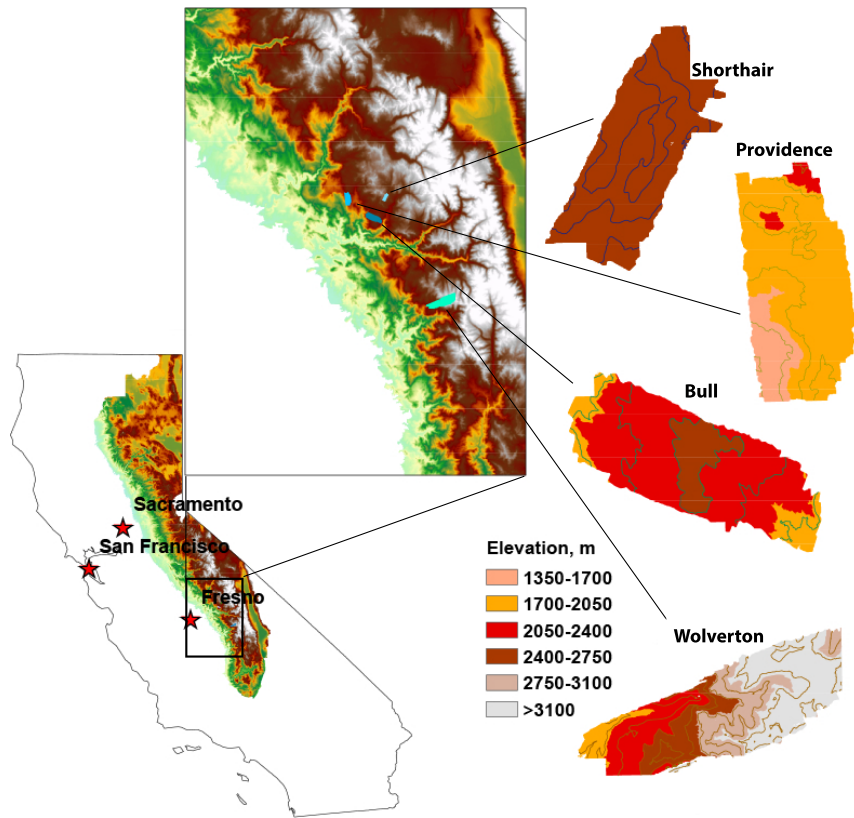
3 Table 3. Linear regression of averaged snow depth vs. elevation in four sites

	Bull	Shorthair	Providence	Wolverton
Open R ²	0.968	0.797	0.931	0.914
Vegetated R ²	0.978	0.737	0.921	0.972
Open slope, cm per 100 m	21.6	16.1	37.8	15.3
Vegetated slope, cm per 100 m	19.9	13.1	26.0	13.4

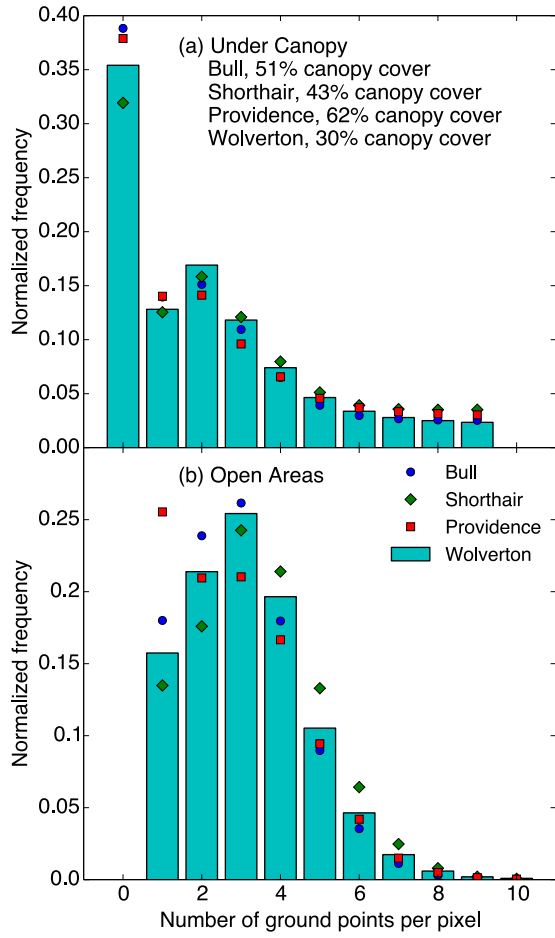
4 Table 4. Coefficients of determination of univariate and multivariate linear models

	Univariate model R^2	Multivariate model R^2
Bull	0.23	0.37
Shorthair	0.06	0.32
Providence	0.39	0.53
Wolverton	0.16	0.38
All sites	0.43	0.57

5



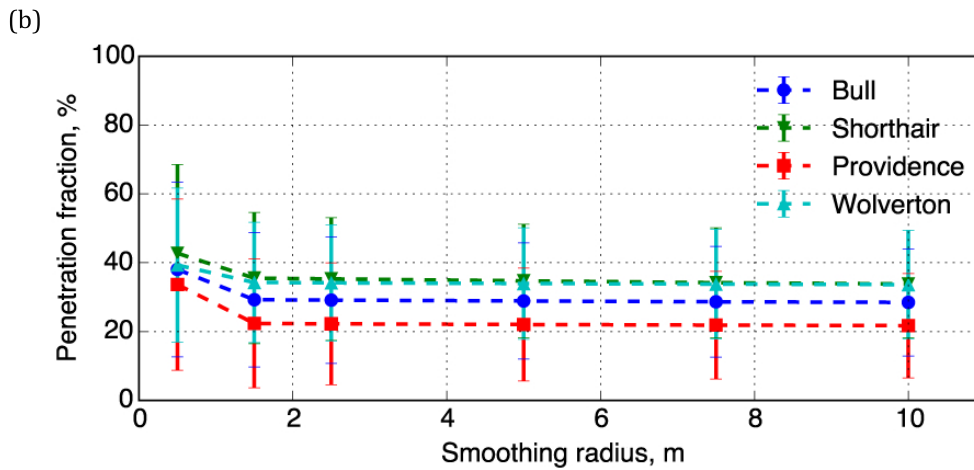
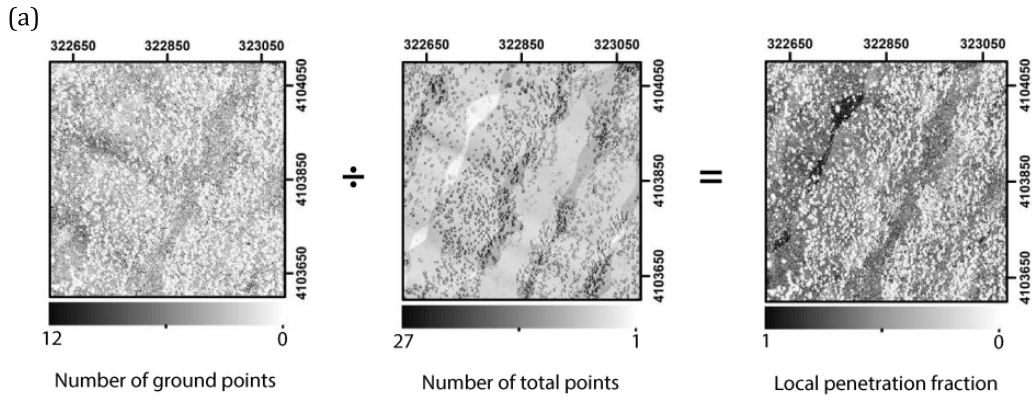
6
 7 Figure 1. Study area and Lidar footprints. (Left) California with Sierra Nevada. (Center) Zoomed view to
 8 show the locations of Lidar footprints. (Right) Elevation and 200-m contour map (100-m for Bull) of
 9 LiDAR footprints



10

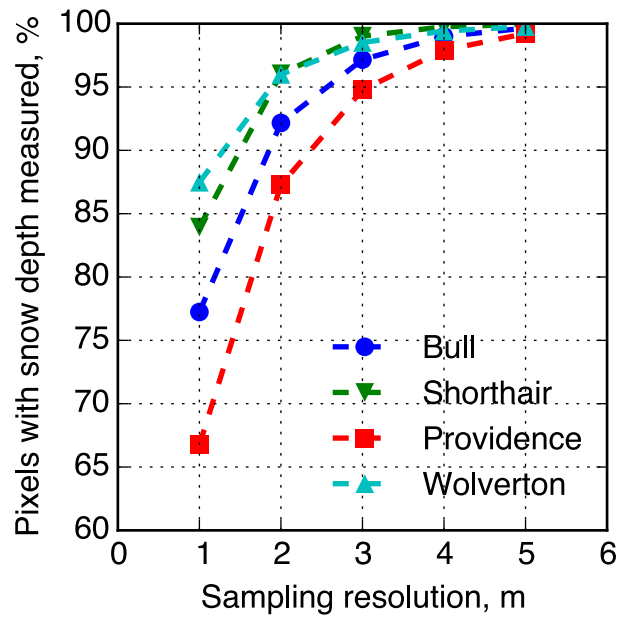
11 Figure 2. (a) Normalized histogram of the number of ground points for under canopy pixels. (b)

12 Normalized histogram of the number of ground points in open pixels.



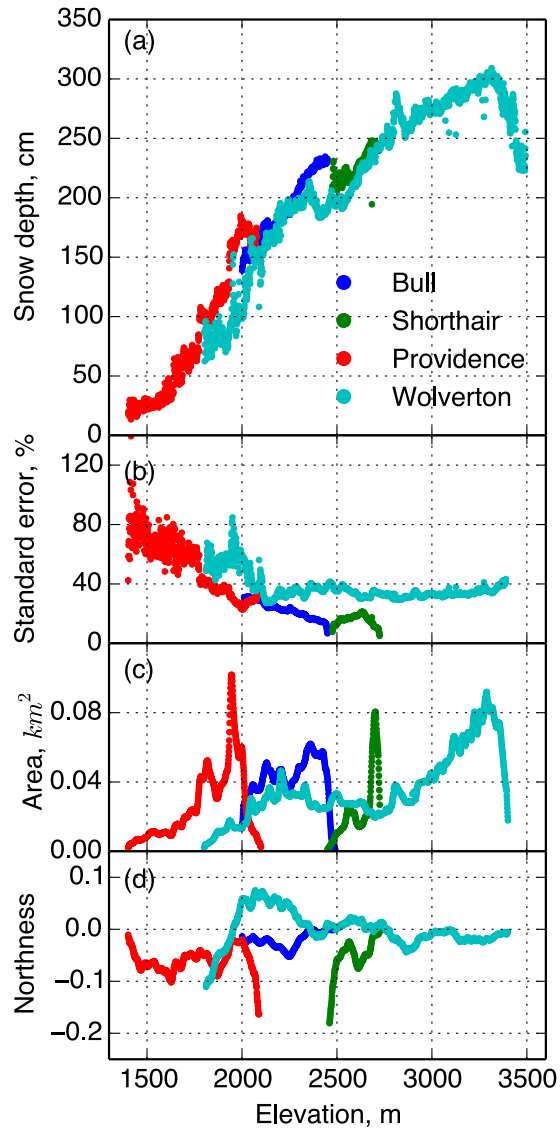
13

14 Figure 3. (a) Dividing the number of ground points of each 1-m pixel by the total number of points in the
 15 pixel will result the penetration fraction of the local pixel. (b) Sensitivity of the smoothed penetration
 16 fraction to the smoothing radius, showing that the result is not sensitivity as the radius is larger than 1.5 m.



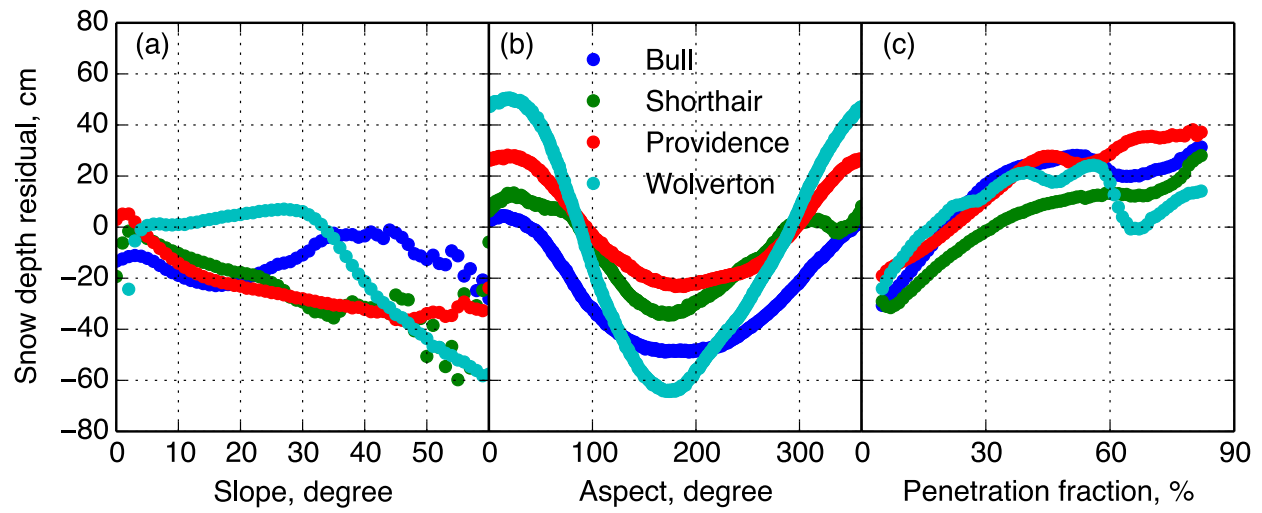
17

18 Figure 4. Sensitivity of the percentage of pixels with snow depth measured to the sampling resolution
 19 used in processing the Lidar point cloud at each site.



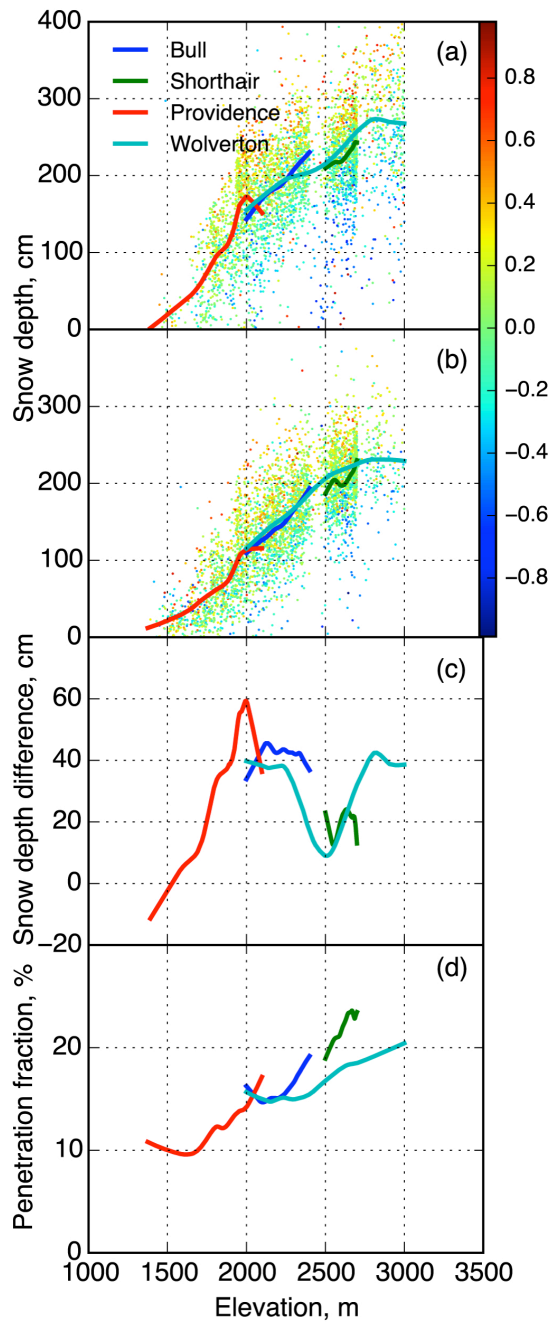
20

21 Figure 5. (a) Averaged snow depth from snow-on and snow-off Lidar data versus elevation for pixels in
 22 the open at the four sites. (b) Standard error of the snow depth within each 1-m elevation band. Values
 23 above 3400 m not shown, where there are few data. (c) Total area of averaged data within each elevation
 24 band. (d) Averaged northness of each elevation band from four sites.



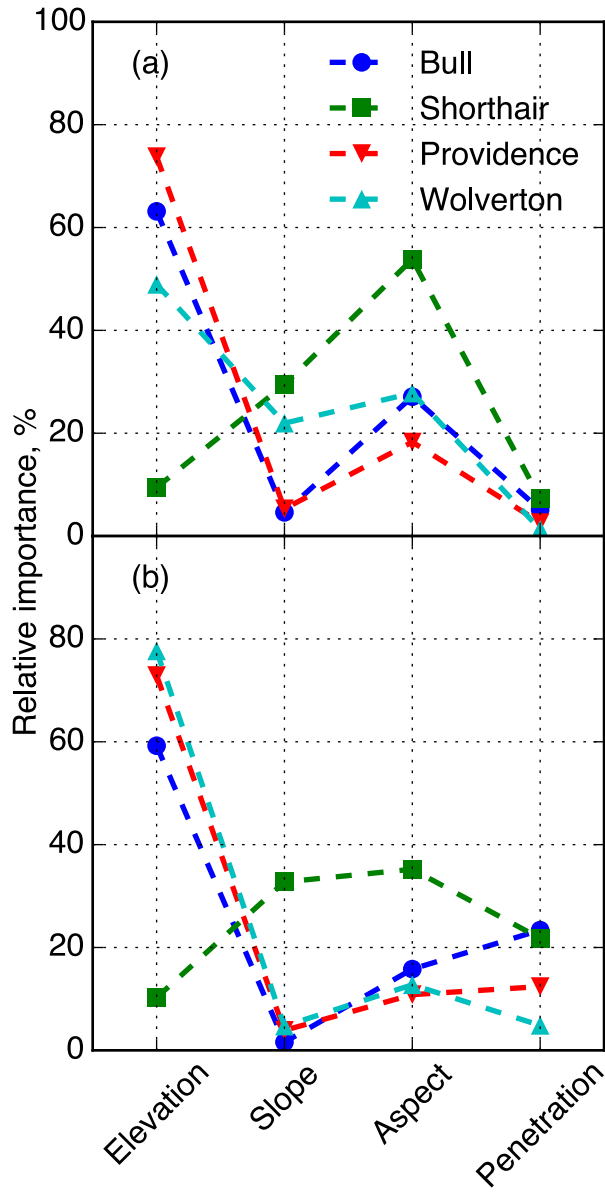
25

26 Figure 6. (a) Averaged snow-depth residual along slope. Raw snow-depth residual was calculated from
 27 Lidar measured snow depth and estimated snow depth from the linear regression model (open areas). (b)
 28 Averaged snow-depth residual along aspect. (c) Averaged snow-depth residual along penetration fraction.



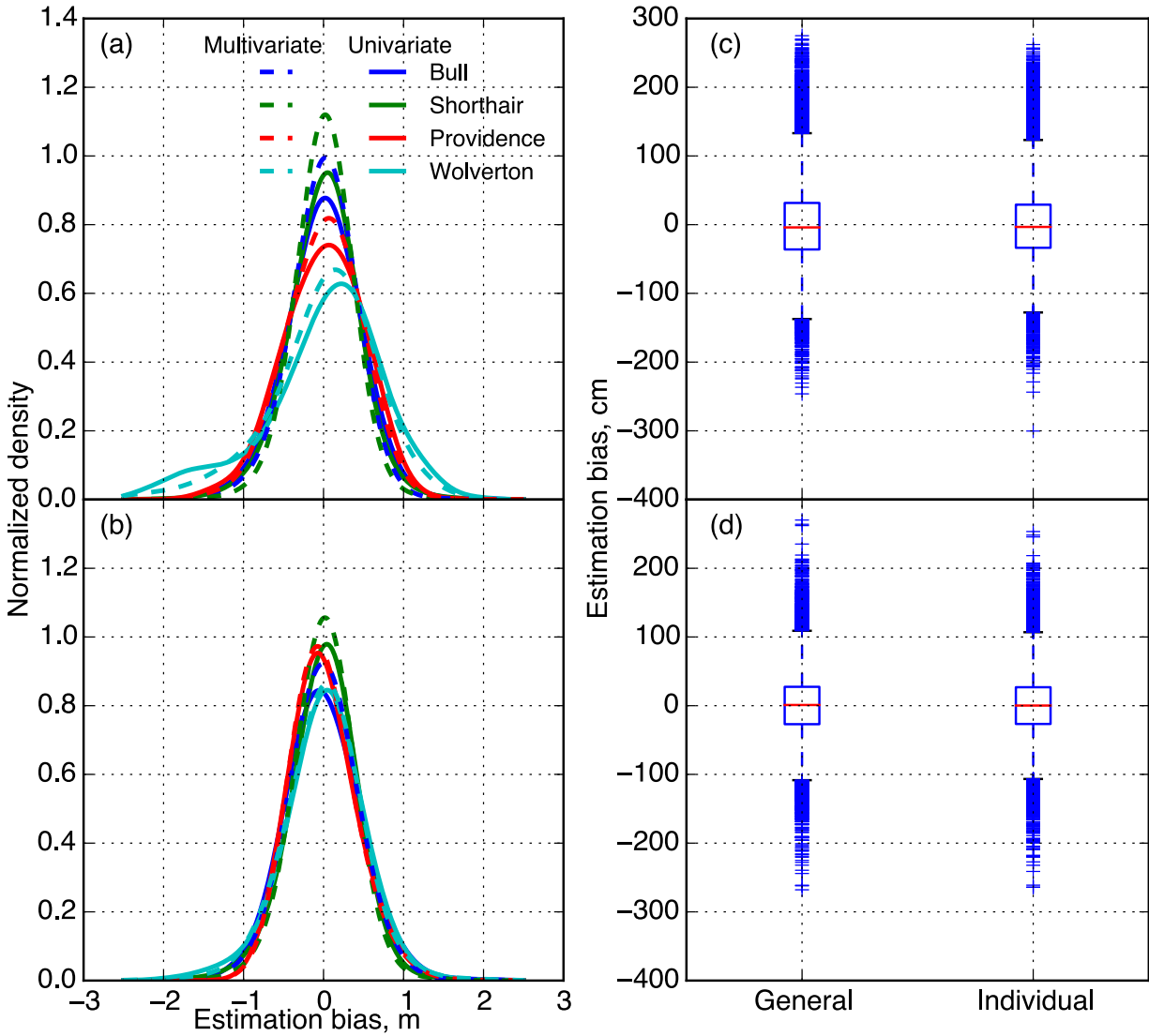
29

30 Figure 7. LOESS smoothed snow depth with northness color coded scatterplot of raw-pixel snow depth
 31 against elevation for (a) open area (b) canopy-covered area. (c) Snow-depth difference along elevation
 32 calculated from the LOESS smoothed snow depth. (d) Averaged penetration fraction.



33

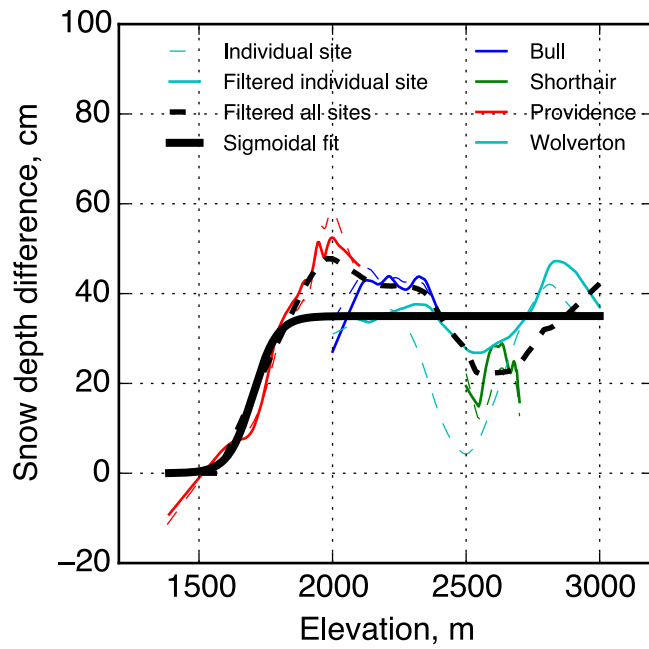
34 Figure 8. Relative importance of each physiographic variable in predicting the snow depth from each site
 35 for (a) open area (b) canopy-covered area



36

37 Figure 9. Normalized density of estimation bias for (a) open area (b) canopy-covered area; Estimation
 38 bias boxplots of using one general linear model with all sites' data combined and four linear models of
 39 each individual site for (c) open area (d) canopy-covered area.

40



41

42 Figure 10. Snow-depth difference between open and canopy-covered area: comparison between
 43 using raw 1-m pixel snow depth and northness-filtered 1-m pixel snow depth, together with the
 44 sigmoidal fit of the snow-depth difference changing with elevation

45